

Rates and controls of acid production in commercial-scale sulphur blocks



Birkham TK^{1*}, Hendry MJ¹, Barbour SL² & Cheema T³

¹Dept of Geological Sciences, University of Saskatchewan, Saskatoon, SK

*Now with O'Kane Consultants

²Dept of Civil and Geological Engineering, University of Saskatchewan, Saskatoon, SK

³Syncrude Canada Ltd., Edmonton, AB

ABSTRACT

Acidic drainage (pH 0.4 - 1.0) from oxidizing sulphur (S⁰) blocks is an environmental concern in regions where S⁰ is stockpiled. In this study, the locations, controls and rates of H₂SO₄ production in commercial-scale S⁰ blocks (~1-2 x 10⁶ m³) in northern Alberta, Canada were estimated. The presence of oxygen (O₂) in the S⁰ blocks is a primary control on S⁰ oxidation; therefore, rates of atmospheric O₂ flux into S⁰ blocks can be used to quantify S⁰ oxidation rates. Analyses of multiple gas species (O₂, N₂, and CO₂) were required to quantify atmospheric O₂ influx. *In situ* modelling of O₂ concentrations ([O₂]) suggested 70 to >97% of the annual H₂SO₄ production occurred in the upper 1 m of the blocks where temperatures increase to >15°C during the summer. Advection, created by O₂ consumption within the block, accounted for 20% of the total O₂ influx and considerably increased H₂SO₄ production in the block above that attributed to O₂ diffusion. S⁰ oxidation was limited by water availability to fracture faces and zones of friable S⁰. A conceptual model of acid transport from the blocks was developed in which fresh infiltrating water mixes with acidic pore-water (mean pH = -2.1) to produce drainage water with pH 0.4 - 1.0. Implications of this research are relevant globally as construction methods and physical properties of S⁰ blocks are similar worldwide.

RÉSUMÉ

Le drainage d'acidic (pH 0.4 - 1.0) d'oxyder le soufre (S⁰) bloque est une inquiétude de l'environnement dans les régions où S⁰ est stocké. Dans cette étude, les endroits, commandes et taux de production H₂SO₄ dans l'échelle commerciale les blocs de S⁰ (~1-2 x 10⁶ m³) dans Alberta du Nord, le Canada a été estimé. La présence d'oxygène (O₂) dans les blocs de S⁰ est un contrôle primaire sur l'oxydation S⁰; donc, les taux de flux d'O₂ atmosphérique dans les blocs de S⁰ peuvent être utilisés pour quantifier des taux d'oxydation S⁰. Les analyses d'espèces multiples du gaz (O₂, N₂ et CO₂) ont été tenues de quantifier l'afflux O₂ atmosphérique. Dans situ posant de concentrations O₂ ([O₂]) a suggéré 70 à > 97 % de la production H₂SO₄ annuelle s'est produit à 1 m supérieur des blocs où les températures augmentent à > 15°C en été. L'advection, créée par la consommation O₂ dans le bloc, a représenté 20 % du total O₂ afflux et production de H₂SO₄ considérablement augmentée dans le bloc au-dessus de cela attribué à la diffusion O₂. L'oxydation de S⁰ a été limitée par la disponibilité d'eau de fracturer des visages et des zones de S⁰ friable. Un modèle conceptuel de transport acide des blocs a été développé dans lequel les mélanges d'eau s'infiltrant frais avec acidic étudient soigneusement - l'eau (voulez dire pH = -2.1) produire l'eau de drainage avec pH 0.4 - 1.0. Les implications de cette recherche sont pertinentes à l'échelle mondiale comme les méthodes de construction et les propriétés physiques de blocs de S⁰ sont semblables dans le monde entier.

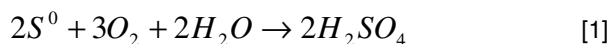
1 INTRODUCTION

Elemental sulphur (S⁰) has been stockpiled over the past 20 years due to a global S⁰ surplus (Ober 2002). Increased S⁰ production at petroleum refineries, natural gas plants, coking plants, and non-ferrous metal smelters (Ober 2008) combined with a decrease in S⁰ prices from \$300 to ~\$25 USD per tonne from 1982 to 2002 has forced tens of Mt to be stockpiled at industrial sites. This is particularly common in more remote regions where transportation costs are relatively high, including northern Canada, the Middle East, and the Caspian Sea region (Proce 2006). Increased demand from 2005-2008 (ERCB 2008) resulted in S⁰ prices as great as \$700 US per t (Kosich 2008) and the re-melting of S⁰ from the most accessible stockpiles. However, a S⁰ surplus and continued stockpiling is expected to continue from 2011-2017 (ERCB 2008).

Canada was the world's largest S⁰-producing country in 2007 (Ober 2008) with 11.6 Mt stockpiled as of April 2008 (ERCB 2008). Bitumen upgrading at oilsands mining operations in northern Alberta resulted in 1.5 Mt of stockpiled S⁰ in 2007 with annual stockpiling expected to increase to 5.3 Mt by 2017 (ERCB 2008).

S⁰ is commonly stored by pouring molten S⁰ (135 to 145 °C) in a confined area on the ground surface where it solidifies (at 115 °C) in lifts approximately 0.1 m thick. Gradually, a large S⁰ block is built up with typical footprint dimensions of 100-200 m and heights of 10-20 m. Some of the stored S⁰ within these above-ground blocks will oxidize to H₂SO₄ (Equation [1]) and this acid is flushed from the blocks as precipitation percolates through the blocks. Most sites more than 20 years old, experience problems with groundwater contamination as a result of S⁰ oxidation to H₂SO₄ (Synchrude 2004a). Drainage water seeping from the base of these S⁰ blocks typically has low pH (0.4-1.0) and high SO₄

concentrations (12,000-34,000 mg/L), and soil and groundwater acidification and soil salinization adjacent to the blocks can be a concern for refinery operators and government regulators.



Oxidation of S^0 to SO_4 (i.e., production of H_2SO_4) is dependent on microbial activity (Janzen and Bettany 1987a), of which O_2 concentration [O_2] is an important control. The objective of this study was to quantify *in situ* H_2SO_4 production rates by modelling *in situ* pore-gas [O_2] distributions in a S^0 block. Modelled H_2SO_4 production was compared with H_2SO_4 loadings in drainage from a S^0 block, and a conceptual model for H_2SO_4 production and transport was developed. Implications for long-term H_2SO_4 production rates and S^0 storage are discussed.

2 FIELD SITE AND S^0 CHARACTERIZATION

The two commercial-scale S^0 blocks in this study were located at the Syncrude Canada Ltd. oilsands mine in northern Alberta, Canada (57°02'34.89"N, 111°38'36.14"W). The Phase 1 block was constructed between 1994 and 2004, was 359 m long and 168 m wide (area at base of 60,312 m²) (Syncrude Canada Ltd. 2004b), and contained an estimated 946,000 m³ of S^0 . The maximum height of this block was 17.5 m at TM03-07 (Figure 1). The Phase 2 block was constructed approximately 100 m west of the Phase 1 block between 1997 and 2005. It was 261 m long and 334 m wide (area at base of 87,174 m²) (Syncrude Canada Ltd., 2004b), had a height of 25 m, and an estimated volume of approximately 2,000,000 m³.



Figure 1. Aerial photo of Phase 1 (lower right) and 2 (upper left, under construction) S^0 blocks at Syncrude Canada Ltd. oil sands mine in 2003. Black dots on the Phase 1 block represent locations of vertically-nested gas sampling ports (SRD series) and thermistors (TM series). The white triangle at the north-east corner of the Phase 2 block represents the location of the weir and drainage sampling location. The dark texturing on the surface of the Phase 1 block is wind-blown sediment.

Dark orange flow channels on the Phase 2 block are molten S^0 . The passageway for the Phase 2 pouring towers divides the block in a north-south direction, while the passageway for the Phase 1 pouring towers has been filled except for a small section at the south end of the block.

Both blocks were constructed using the same method whereby molten S^0 was poured from three towers into two areas on both sides of the towers (east and west directions). The extent of the molten ($\sim 135^\circ\text{C}$) S^0 flow was constrained by aluminum forms and the S^0 block gradually built up as sequential lifts (<0.1 m thick) of molten S^0 solidified ($<115^\circ\text{C}$). After the S^0 reached the desired final height, the pouring towers were dismantled and S^0 was poured into the passageway between the east and west blocks.

Mean annual precipitation (water equivalent) at Fort McMurray (40 km south of S^0 blocks) is 455.5 mm, with 342.2 mm as rainfall and the remainder as snow (annual data from 1971-2000; Environment Canada, 2009a). The mean annual temperature is 0.7°C , with the lowest monthly mean in January (-18.8°C) and the highest in July (16.8°C).

3 BACKGROUND S^0 CHARACTERIZATION

Extensive fracturing of S^0 blocks occurs due to 12.5% volume shrinkage during solidification and mineral changes (Bonstrom, 2007). Bonstrom (2007) measured a fracture porosity (n_f) of 1.4%, a mean S^0 matrix porosity (n_m) of 9.3% ($n = 280$, s.d. = 3.4 %), an effective (interconnected) n_m of 6.5%, and mean vertical and horizontal fracture frequencies of 33.5 and 5.4 m⁻¹, respectively. Because S^0 is hydrophobic, pressure heads of 1-2 m are required for water to begin to enter the pore spaces of unfractured (matrix) S^0 .

Birkham et al. (2010a) reported that water flow and storage in S^0 blocks was limited to discrete fractures and zones of friable S^0 . Hydrophilic conditions developed on fracture faces in areas of microbial colonization which created preferential pathways for rainfall infiltration and storage. A dye tracer test provided visual evidence of the preferential infiltration pathways (Figure 2). Water did enter the matrix S^0 porosity in the bottom 2 m of the block where ponded conditions resulted in positive pore-water pressure heads as great as 2.5 m. The mean volumetric moisture content of the unsaturated portion of Phase 1 block was 0.6% ($n=108$, s.d.=0.7%; Birkham et al., 2010a). Percolation into the geologic media underlying the blocks was a minor component of the water balance as greater than 95% of precipitation falling on the blocks rapidly infiltrated through the block and then drained horizontally through the base of the blocks, or evaporated from the surface of the blocks (Birkham et al., 2010a). Water that drained horizontally through the base of the blocks was channelled to collection ditches containing mine process water and recycled as part of the site's overall water treatment process.

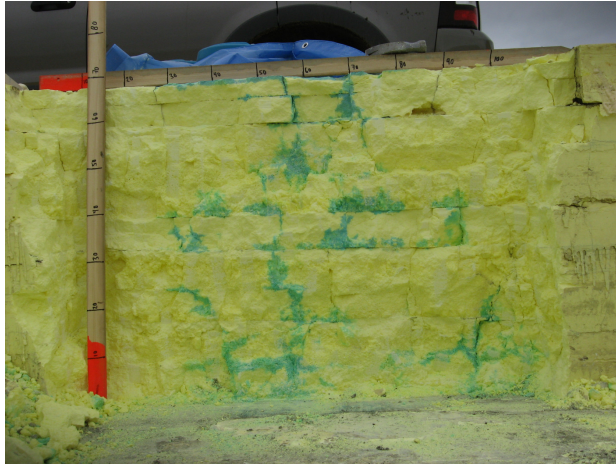


Figure 2. Excavated vertical cross-section of S⁰ block below area of dye tracer infiltration.

Gas diffusion transport parameters were quantified through unfractured S⁰ using laboratory diffusion cells and for *in situ* conditions by an SF₆ tracer experiment in the Phase 1 block. Gas diffusion was quantified according to Fick's law:

$$J_i = -\theta_a \omega D_{air} \frac{dC_i}{dz} \quad [2]$$

where J_i is the mass flux of species i (MT⁻¹); θ_a is the air-filled porosity; ω is the relative gas diffusivity (dimensionless; Moldrup et al., 2004), which is <1 and related to the tortuosity (τ) of the porous medium (ratio of gas particle path length to straight-line travel distance); C_i is the concentration of species i (M·L⁻³); z is the distance in the direction of the mass flux (L); and D_{air} is the diffusion coefficient of the species in free air (L²·T⁻¹). D_{air} for O₂ is 1.78 × 10⁻⁵ m²·s⁻¹ (Weast and Astle, 1981).

The effective gas diffusion coefficient (D_e) was defined by:

$$D_e = \omega D_{air} \quad [3]$$

Values of ω × θ_a averaged 0.0067 for unfractured S⁰ and approximately 0.015 for fractured S⁰. An equivalent porous medium (EPM) approach was used for modelling gas diffusion through fractured S⁰ where contributions of the matrix and fracture porosity to the ω were weighted proportionally to their percentage of the total porosity. Diffusive O₂ influx accounted for ~80% of the total O₂ influx, with advective influx accounting for 20% (Birkham et al., 2010b). Advective influxes along total pressure gradients were the result of net loss of gas volume due to O₂ consumption without the production of a replacement gas of equivalent volume.

Temperatures in the Phase 1 block were variable with time in the upper 5 m (range of -18 to 25 °C at 0.5 m depth), and uniform with depth below 5 m (average internal temperature of 11.1 °C) (Birkham et al., 2010c). S⁰ oxidation rates measured in lab cells were more

sensitive to temperature (Q₁₀=4.3) than typical soil respiration rates, were low (but measureable) at a temperature of 2.9 °C, and independent of [O₂] for [O₂] >1%. S⁰ oxidation in the lab cells was mediated by autotrophic S⁰-oxidizing bacteria which consume both O₂ and CO₂. CO₂ consumption rates by the autotrophic bacteria were less than the detection limit and estimated to be less than 6% of the O₂ consumption rates (Birkham et al., 2010c).

4 MATERIALS AND METHODS

4.1 Drainage volumes and snow-water equivalent

Hourly outflow rates at the Phase 2 block were measured in 2006 using a V-notch weir (Figure 1) as described by Birkham et al. (2010c). The water equivalent of the snowpack on the Phase 1 block was estimated from the results of a snow depth/density survey on 13 March 2006 at 57 locations along two transects.

4.2 pH and SO₄ concentrations of drainage water

Drainage water samples (n=33) from the Phase 2 S⁰ block were collected from 24 April to 9 October 2006 with an automated ISCO® water sampler in 1 L plastic bottles for pH and SO₄ concentration [SO₄] measurements. The mean sampling interval was 6 days and ranged from 1-50 days. Although the plastic bottles in the automated water sampler were left uncapped for up to two months (within an enclosed container), and the time between sample collection and pH and [SO₄] measurements was as great as three months (samples were stored in refrigerated, sealed 1 L plastic bottles), the delay in measurement had a minimal effect on pH. Analyses on selected samples at elapsed times of 1 h to 90 d between sample collection and pH measurement show the pH change was within the measurement error (±0.3 pH units, see below) (data not presented).

pH was measured using a Thermo Orion® 250A pH meter and a mV calibration (for dilute H₂SO₄ solutions with pH of -0.27, 1.0 and 2.0). The pH of each field sample (±0.3 pH units) was determined by measuring the mV of the sample and linearly interpolating a pH value from the calibration data. [SO₄] was measured on samples using a Dionex® ion chromatograph. Accuracy of [SO₄] analysis (including dilutions up to 500× and chromatograph error) was ±10%.

4.3 In situ relative humidity distribution

Relative humidity (RH) and temperature were measured in gas samples collected within the Phase 1 S⁰ block on 16 May 2007 at SRD05-142, SRD05-143, and SRD05-144 (Figure 1). Samples were collected in 60-mL syringes from vertically nested gas sampling ports (CMT channels, installation details described below) after purging 100 mL of gas for every meter of channel using a 140-mL syringe fitted with a three-way luer-lock valve. Using a flow-through technique with care taken to avoid atmospheric contamination (described in detail in

Birkham et al., 2010b), temperature and RH of the samples were measured with a Digi-Sense® RH meter. RH accuracy was $\pm 2\%$ between 10 and 90%, and $\pm 4\%$ between 0-10 and 90-100% RH; temperature accuracy was $\pm 0.2\%$. RH measured on samples collected above-ground was corrected to in situ temperatures measured at TM03-01, -04, and -07 (Figure 1) using the method presented by Birkham et al. (2010c). The error in calculated in situ RH was estimated to be $\pm 3\text{-}5\%$ (actual RH value, not a percentage of RH) for an error in in situ temperature of $\pm 1^\circ\text{C}$, and approximately $\pm 20\%$ for a temperature error of $\pm 4^\circ\text{C}$.

4.4 In situ $[\text{O}_2]$, $[\text{N}_2]$, and $[\text{CO}_2]$

Vertically nested gas sampling ports along the SRD05/SRD06 transect on the Phase 1 block (Figure 1) were installed to measure $[\text{N}_2]$, $[\text{O}_2]$, and $[\text{CO}_2]$ profiles at depths of 1-15 m for the SRD05 series and 0.5-6 m for the SRD06 profile. Sampling port construction and installation are described Birkham et al. (2010c). In situ $[\text{O}_2]$, $[\text{N}_2]$, and $[\text{CO}_2]$ were measured on 9 December 2005, and 11 March, 17 May, and 12 September 2006. Sampling methodology and analytical techniques are described in Birkham et al. (2010c).

4.5 $[\text{O}_2]$ distribution modelling

$[\text{O}_2]$ distributions in the Phase 1 block were modelled to estimate the location and rates (per unit volume, β_{O_2}) of O_2 consumption. The aim of the modelling was to simulate general trends in the $[\text{O}_2]$ distribution, rather than exactly match the modelled and measured $[\text{O}_2]$ contours. The modelled β_{O_2} were used as an estimate of H_2SO_4 production rates according to the stoichiometry in Equation [1]. The 2-D modelling was performed using the Geostudio® 2007 numerical modelling suite, which included coupled models for advective gas flow (SEEP/W®) as well as gas reaction rates and diffusive fluxes (CTRAN/W®). Birkham et al. (2010b) used this same approach to model steady-state late-summer $[\text{N}_2]$, $[\text{O}_2]$, and $[\text{CO}_2]$ distributions in the Phase 1 block. To meet the objective of this paper, we focus on seasonal trends in $[\text{O}_2]$ and further examine the controls on *in situ* $[\text{O}_2]$. The reader is referred to Birkham et al. (2010b) for details on model grid refinement, and theoretical equations describing gas diffusion and advection. In summary Fick's (Eqn. [2]) and Darcy's laws were used to describe diffusive and advective gas transport, respectively.

An EPM approach was assumed to represent the fractured S^0 blocks with the EPM air-filled porosity (θ_a) and ω ranging from 6.7% and 0.13, respectively, for depths from 8-17 m, and as great as 9.4% and 0.44 in the upper 8 m (Birkham et al., 2010b).

Winter $[\text{O}_2]$ cross sections were modelled using the steady-state summer $[\text{O}_2]$ as initial conditions and varying the O_2 consumption rate per unit volume (β_{O_2}) within the block to correlate with in situ winter temperatures. A surficial layer (0.05 m thickness) with relatively low EPM θ_a and ω was added to the winter

model to simulate a surficial ice/snow layer (discussed below).

5 RESULTS AND DISCUSSIONS

5.1 Environmental loading of H_2SO_4

Concentrations of SO_4 and pH of drainage water from the Phase 2 block (Figure 3) ranged from 13-33 $\text{g}\cdot\text{L}^{-1}$ and 0.4-1.0, respectively. The greatest $[\text{SO}_4]$ and smallest pH values were measured from late May to early July. $[\text{SO}_4]$ decreased to $< 20 \text{ g}\cdot\text{L}^{-1}$ and pH increased to > 0.65 proceeding heavy rainfall and high drainage outflow rates in mid-July. Measured pH and $[\text{SO}_4]$ matched theoretical values calculated using the computer program PHRQPITZ, which uses the Pitzer method and the MacInnes convention for scaling individual ion activity coefficients (Plummer et al., 1988). For example, theoretical pH from 0.45-0.83 corresponded to $[\text{SO}_4]$ from 15-35 $\text{g}\cdot\text{L}^{-1}$, which are similar to measured values. This validated the analytical methods used for measuring pH and $[\text{SO}_4]$, and suggested the acidity in the S^0 block drainage was from H_2SO_4 .

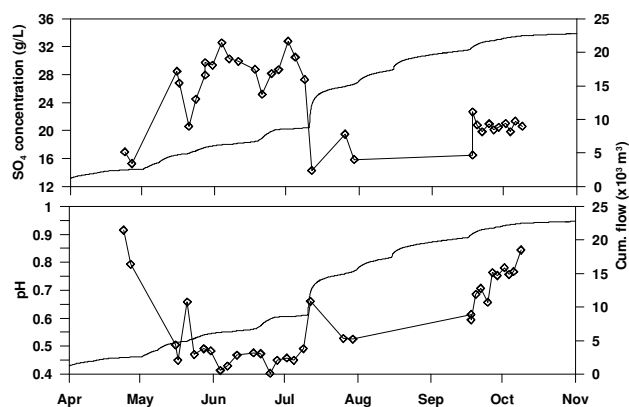


Figure 3. $[\text{SO}_4]$ (A.) and pH (B.) (symbols), and cumulative flow volumes (line) of drainage water from the Phase 2 S^0 block for the 2006 field season.

The cumulative mass of SO_4 in drainage from the Phase 2 block was estimated to be $4.6 \times 10^5 \text{ kg}$ ($1.5 \times 10^5 \text{ kg S}^0$) between 24 March and 2 November 2006. Daily loadings of $[\text{SO}_4]$ were estimated by multiplying the measured daily flow volume by the $[\text{SO}_4]$. On days not measured, $[\text{SO}_4]$ was estimated by linear interpolation. SO_4 loading from 24 March to 2 November 2006 from the Phase 1 block was estimated at $3.1 \times 10^5 \text{ kg}$ ($1 \times 10^5 \text{ kg S}^0$) by scaling the Phase 2 loading by 0.67 (the ratio of Phase 1 to Phase 2 footprint areas). Drainage was observed in late winter and early spring (during snowmelt) when flow measurements were not being recorded due to snow and ice buildup at the weir. The SO_4 loading during this time was estimated to be $6.2 \times 10^4 \text{ kg}$ ($2.1 \times 10^4 \text{ kg S}^0$) assuming an $[\text{SO}_4]$ of $20 \text{ g}\cdot\text{L}^{-1}$ and a drainage volume from snowmelt on the Phase 1 block of $3,100 \text{ m}^3$. The snowmelt water volume was estimated using a mean snow depth of 184 mm ($n=57$,

s.d.=51 mm), and mean snow density of 280 kg · m⁻³ (n=8, s.d.=66 kg · m⁻³). The total SO₄ loading estimate for 2006 from the Phase 1 block was 3.7 × 10⁵ kg (1.2 × 10⁵ kg S⁰). Assuming the Phase 2 block had similar snowpack depth, the estimated 2006 SO₄ loading for the Phase 2 block was 5.5 × 10⁵ kg (1.8 × 10⁵ kg S⁰).

The cumulative SO₄ loading from the Phase 2 block increased linearly with cumulative outflow volume (R²=0.996, not presented), suggesting the production and removal rates of SO₄ were approximately equal from late March to November of 2006. These data for a one-year time period were not sufficient to conclude if H₂SO₄ production rates had reached a long-term steady state as H₂SO₄ production rates may be gradually increasing with time (discussed below). To observe an increase in the slope of the cumulative SO₄ loading vs. outflow volume curve (i.e., generally increasing trend in outflow [SO₄], or decreasing trend in outflow pH), measurements of [SO₄] and outflow rates over many years may be required. Assuming H₂SO₄ in outflow waters resulted from partial mixing of infiltrating water (containing negligible H₂SO₄) and resident water in the S⁰ block, [SO₄] would be greater (and pH less) *in situ* than in drainage water. This is discussed in greater detail below.

5.2 In situ relative humidity distribution

RH within the S⁰ block ranged from 40-100%, with a mean of 68% (s.d.=17%, n=21). RH values less than 100% in unsaturated porous media can result from total suction (the sum of matric and osmotic suction) greater than 3,000 kPa (Fredlund and Rahardjo, 1993; Wilson et al., 1997). Matric suction values likely did not exceed 3,000 kPa given that S⁰ itself is hydrophobic and consequently has little capacity to exhibit capillarity, and that free-water is present at the bottom of the Phase 1 S⁰ block (total depth of approximately 17 m; Birkham et al., 2010a). For comparison, Severinghaus et al. (1996) concluded RH in 100-m thick unsaturated sand dunes in an arid environment was at 100% at depths as shallow as 0.2 m.

Based on these data, RH values <100% were attributed to osmotic suctions resulting from concentrations of dissolved solids (i.e., H₂SO₄) within the block. RH values of 40% (lowest measured *in situ* RH) and 68% (mean measured *in situ* RH) correspond to H₂SO₄ concentrations (weight %) of 47.5% and 33.7%, respectively (Wilson, 1921). Using the PHRQPITZ program, pH values of -3.8 and -2.1 were calculated for H₂SO₄ concentrations of 47.5 and 33.7%, respectively. Although additional testing is required, these data suggest *in situ* pH values at least for some areas in the Phase 1 S⁰ block (S⁰ oxidation sites on fracture faces and areas of friable S⁰, Birkham et al. 2010a) were considerably lower than the pH of the drainage water, and that the H₂SO₄ in the drainage waters was the result of mixing of resident (lower pH) water in the S⁰ block with fresher (higher pH) infiltrating water. Assuming a simple mixing model whereby infiltrating water (with [SO₄]=0) mixes with *in situ* water (with an average [SO₄]=390 g · L⁻¹, equivalent to pH=-2.1) to produce drainage water from

the blocks with [SO₄] from 15-32 g · L⁻¹ (Figure 3), the percentage of resident water in each liter of drainage water was estimated to be 4-8%, respectively. Mixing ratios from 4-8% would result in 18-36 L of resident water (per m²) mixing with infiltrating precipitation each year (assuming total annual precipitation of 455.5 mm). This is approximately 18-35% of the total volume of stored water in the Phase 1 block (102 L per m², assuming a height of 17 m and a volumetric moisture content of 0.6%). The effect of the low pH of resident water on microbial activity is discussed below.

RH of 100% at depths of 1 and 5 m at SRD05-144B corresponded to the increased moisture content measured at SRD05-144 at depths of 1.2 and 5 m (Birkham et al., 2010a). However, the 100% RH measured at 1 m depth at SRD05-143 did not correlate with moisture content measured by Birkham et al. (2010a) and was attributed to heterogeneity in the moisture distribution within the S⁰ block. Moisture content samples in Birkham et al. (2010a) were collected from a borehole about 3 m away from the nested gas sampling ports used for the RH measurements.

5.3 Measured and modelled distributions of *in situ* [O₂]

Trends in measured [O₂] distributions in the Phase 1 S⁰ block for four sampling dates in 2006 are presented in Figure 4. [O₂] varied by 3-5% throughout the year with the lowest and highest levels measured in September and March 2006, respectively. General trends in [O₂] were similar throughout the year, with steep vertical gradients near the top surface of the block and more gradual lateral gradients.

Birkham et al. (2010b) assumed the late-summer [O₂] distribution represented quasi-steady state conditions and modelled this distribution (Figure 5A) by applying O₂ consumption rates (β_{O₂}) of 0.68 mol O₂ m⁻³ · d⁻¹ in the upper 1 m and <2.7 × 10⁻⁴ mol O₂ m⁻³ · d⁻¹ in the rest of the S⁰ block (where [O₂] was >0) for EPM θ_a and ω of 7.3% and 0.21, respectively. θ_a and ω were 9% and 0.44, respectively, in the outer 35 m for depths of 0-1.5 m. Assuming a possible range in EPM θ_a and ω from 6.7% and 0.13 to 9% and 0.44, the range in best-fit β_{O₂} in the upper 1 m was from 0.39-1.8 mol O₂ m⁻³ · d⁻¹.

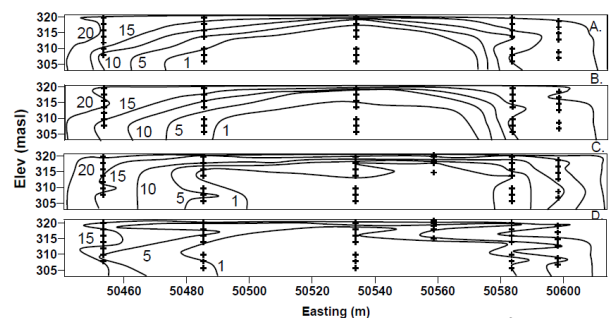


Figure 4. [O₂] cross sections in the Phase 1 S⁰ block for A) December 2005, B) March 2006, C) May 2006, and D) September 2006. Contours of 20 and 10% in Figure 4D

have been omitted to improve clarity. Cross symbols represent sampling ports in the S⁰ block.

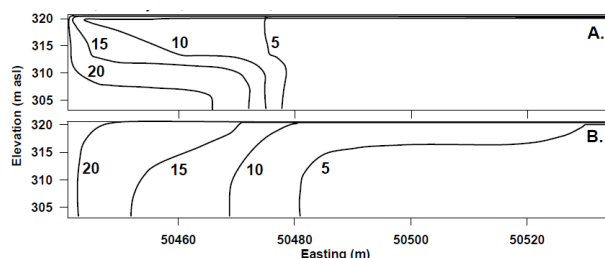


Figure 5. Simulated [O₂] distributions for Phase 1 S⁰ block, where the left side of the cross section is the west side of the block, and the right side of the cross section is the middle of the pouring tower alley (symmetry assumed). Modelled distributions are for: A) summer conditions with increased β_{O_2} in the upper 1 m (i.e., steady-state late summer conditions), and B) steady-state winter conditions with a uniform β_{O_2} applied throughout the block (β_{O_2} from 0-1.5 m set to zero) assuming Figure 5A as initial conditions.

The increased β_{O_2} near the top surface was required to create steep vertical O₂ gradients in the upper 1 m. We hypothesized greater β_{O_2} during the summer near the S⁰ block surface was the combined result of temperatures greater than 10°C for approximately 120 d during periods of greater solar radiation and air temperature (Birkham et al., 2010c), greater microbial activity (Pisz, 2008; discussed below), greater availability of nutrients from wind-blown sediments on the surface of the block, and more accessible S⁰ fracture faces (reaction sites). We further hypothesized the fracture frequency and aperture to be greatest near the surface of the S⁰ block (i.e., increased O₂ availability), as pouring of molten S⁰ during block construction remelts underlying S⁰ and reduces the n_f (Syncrude Canada Ltd., 2004b). Sulphur on the surface was commonly observed to be highly fractured and in loose shattered pieces as thick as 0.15 m.

Pisz (2008) collected samples from depth intervals of 0-0.1, 0.4-0.5, 0.9-1.0, 1.9-2.0, 2.9-3.0, 4.9-5.0, and 5.9-6.0 m at SRD05-143, -144, and -145 for microbiological analyses. Using the MPN technique, resident bacteria were only detected in the samples from 0-0.1 m at average concentrations of 18 MPN g⁻¹ S⁰ for culturable autotrophic S⁰ oxidizers and 3 MPN g⁻¹ S⁰ for thiosulphate (S₂O₃) oxidizers. Pisz (2008) also detected the greatest concentration of *A. thiooxidans* from 0-0.1 m using polymerase chain reaction and DNA sequencing; however, these concentrations were not statistically different than for greater depths. S⁰-oxidizing microorganisms commonly occur in soils (Lawrence and Germida, 1988), therefore the source of microorganisms was assumed to be wind-blown sediments that were deposited on top of the block and transported into the block by infiltrating water.

[O₂] distributions in the late winter (Figure 5B) were modelled by removing the increased β_{O_2} in the upper 1 m, as temperatures at depths <1.5 m were <5°C

(negligible β_{O_2}). However, simply removing the increased near-surface β_{O_2} resulted in modelled [O₂] being much too high near the upper surface of the block. Application of a thin (50 mm) layer with low θ_a (5%) and ω (5.6×10^{-5} - 4.5×10^{-2}) on top of the S⁰ block was required to limit influx of atmospheric O₂ and lower modelled [O₂] in the block (Figure 5B). For comparison, typical values of θ_a for sea ice range from 1-5% (Moslet, 2007); Ikeda-Fukazawa et al. (2005) approximated the ω of solid ice to be 2×10^{-6} . The addition of the thin surficial layer represented ice and snow on the top surface of the S⁰ and acted as a barrier to the influx of atmospheric O₂. A thin layer of ice on the surface of the Phase 1 S⁰ block was commonly observed during the winters of 2004 and 2005 (up to 0.02 m thick) and could act as low ω barrier. Mean snowpack depth was 184 mm in March 2006.

The ω for the 50 mm ice/snow layer was decreased with increasing distance from the edge of the block. Best-fit ω values were 4.5×10^{-2} , 5.6×10^{-3} , and 5.6×10^{-5} for easting intervals of 50441-50471 m, 50471-50528 m, and 50528-50538 m, respectively. The decreasing ω with increasing distance from the edge of the block may have been the result of denser or thicker snow/ice pack near the center of the block. Simulations for winter conditions with increased β_{O_2} from 3-3.5 m (where temperatures during winter were >5°C) were simulated but resulted in a poor match with measured [O₂] gradients in the outer 60 m of the block. An air permeability (k_{air}) of 3×10^{-10} m x s⁻¹ was assumed for the winter surficial layer, and 3×10^{-7} m·s⁻¹ elsewhere (estimate based on permeability measurements by Bonstrom (2007) for matrix S⁰).

In spite of the differences between modelled and measured [O₂] contours for late-summer months (Figures 5A and 4D), the general trend was similar. In particular, the 'bending' of measured [O₂] contours towards the outer edge of the S⁰ block during the summer could be simulated by applying increased β_{O_2} values from 0-1 m.

5.4 Comparing O₂ consumption and H₂SO₄ production rates

Annual SO₄ production estimates based on the O₂ modelling for the Phase 2 block are presented in Table 2 (using stoichiometry from reaction [1]). Greater than 97% of the annual SO₄ production was accounted for by assuming a constant β_{O_2} for S⁰ oxidation in the upper 1 m during the summer. However, if a lower β_{O_2} , instead of a greater θ_a and ω , was assumed in the upper 1 m for the outer 35 m of the block (discussed above), S⁰ oxidation in the upper 1 m could account for as little as 70% of annual SO₄ production. The total annual SO₄ production estimated from [O₂] simulations (2.7×10^5 - 1.2×10^6 kg, assuming uniform β_{O_2} in the upper 1m) was 50-220% of the measured mass loading of SO₄ from the Phase 2 block (5.5×10^5 kg). Considering the range and error associated with these estimates, the SO₄ production estimate from the [O₂] modelling was similar to the measured SO₄ mass loading. This was consistent with the linear relationship between cumulative SO₄

loading and outflow (Birkham et al., 2010c) that suggested the production and removal rates of SO_4 were similar in 2006.

Although the β_{O_2} was applied uniformly to each m^3 in the model, data presented above showed O_2 consumption (and H_2SO_4 production) in the blocks was isolated to S^0 surface areas in contact with liquid water. Birkham et al. (2010a) reported the flowpaths for water in the Phase 1 S^0 block were limited to fractures and areas of highly porous or friable S^0 . The reactive surface area in the S^0 block (per m^3) was estimated by dividing the modelled β_{O_2} by a lab-measured α_{O_2} (O_2 consumption rate per m^2 , scaled for the appropriate temperature, Birkham et al., 2010c). For the interior of the S^0 block (at an average temperature of 11.1°C), the reactive surface area estimate was less than $4 \text{ m}^2 \cdot \text{m}^{-3}$. During the summer months, the reactive surface area of the near-surface reactive layer (upper 1 m at an average temperature of 14°C) was estimated at $400\text{-}4,000 \text{ m}^2 \cdot \text{m}^{-3}$. Assuming smooth fracture surfaces at vertical and horizontal frequencies of 33.5 and 5.4 m^{-1} , respectively (Bonstrom, 2007), the fracture surface area was estimated at $145 \text{ m}^2 \cdot \text{m}^{-3}$. This suggested crushed or powdered S^0 particles in addition to discrete fracture faces contributed to available surface area for S^0 oxidation in the upper 1 m.

6 IMPLICATIONS

6.1 Evolution of long-term H_2SO_4 production

S^0 oxidation will result in the gradual consumption or removal of S^0 from the blocks and potentially, the buildup of H_2SO_4 in the S^0 block pore-water. The implications of these processes are discussed below.

6.1.1 Lower pH limit for S^0 oxidation

If the pH of pore-water in the S^0 blocks decreases with time, presumably a lower pH limit for microbially mediated S^0 oxidation will be reached. However, the lower pH limit for microbial S^0 oxidation is not known. Brock (1978) reported microbial growth in water with pH as low as zero. Nordstrom et al. (2000) measured the lowest known pH (to our knowledge) of -3.6 ($[\text{SO}_4]$ as great as $760 \text{ g} \cdot \text{L}^{-1}$) for mine waters in contact with sulphide-rich rock; however, they were not able to determine if viable microbes were present in the water. However, Baker et al. (2004) and related publications demonstrate a complex microbial community in the Richmond Mine waters and biofilms at pH $0.5\text{-}0.9$ that included autotrophic and heterotrophic bacteria, fungi, and protozoa.

If future H_2SO_4 production is limited by acidity, infiltration rates through the blocks will be a key control on the permanence of low pore-water pH in the blocks. H_2SO_4 in the pore-water of blocks with high infiltration rates would eventually be flushed from the block and the effect of low pH on H_2SO_4 production would subside. Conversely, long-term S^0 oxidation rates in blocks stored with cover systems to limit infiltration may decrease with

time as the low pH limit is reached and sustained due to low flushing rates.

6.1.2 Increased porosity with S^0 consumption

S^0 oxidation will gradually decrease the mass of S^0 in the blocks, and increase the porosity of the blocks. Increased porosity will increase both $\omega \times \theta_a$, and the permeability of the blocks, and subsequently increase O_2 and water influx and H_2SO_4 production rates. Assuming β_{O_2} values ranging from $0.39\text{-}1.8 \text{ mol O}_2 \text{ m}^{-3} \cdot \text{d}^{-1}$ ($0.26\text{-}1.2 \text{ mol S}^0 \text{ m}^{-3} \cdot \text{d}^{-1}$) and a S^0 density of $2070 \text{ kg} \cdot \text{m}^{-3}$, the estimated annual S^0 loss to oxidation was $5 \times 10^{-4}\text{-}2 \times 10^{-3} \text{ m}^3$ ($1\text{-}4.6 \text{ kg S}^0$) per m^3 in the upper 1 m. If this mass loss was derived from the fracture faces and translated directly to an increase in n_f , the maximum estimated annual increase in n_f would be $0.05\text{-}0.2\%$. The n_f in the upper 1 m is expected to increase over time as a result of S^0 oxidation; however, recurrent increases in the n_f by $0.05\text{-}0.2\%$ each year will depend on whether fractures close as mass is lost to oxidation (e.g., due to overburden or confining pressures) or if fractures remain 'open'.

6.2 Long-term storage

Minimizing H_2SO_4 production rates for long-term storage of S^0 may include temperature control, biocide application, or reduction of O_2 and water influx. Some implications for these storage options are discussed below.

6.2.1 Water availability

Based on S^0 oxidation rate estimates by Birkham et al. (2010c) ($1.8 \text{ mol O}_2/\text{m}^3/\text{d}$ in the upper 1 m, and $2.7 \times 10^{-4} \text{ mol O}_2/\text{m}^3/\text{d}$ below 1 m), annual water consumption in the Phase 1 block per m^2 was estimated at 2.6 L (depth of 2.6 mm), with 70 to $>97\%$ of the annual water demand occurring in the upper 1 m during the summer. This was only 0.6% of the mean annual precipitation (water equivalent of 455.5 mm ; Environment Canada online data from 1971-2000, www.ec.gc.ca), suggesting that cover systems designed to minimize water infiltration, and thereby minimize H_2SO_4 production in S^0 blocks, would need to be much more effective (efficiency $>99.4\%$) than current conventional cover designs for mine closure (typical efficiency $\sim 95\%$; M. O'Kane, personal communications) to decrease S^0 oxidation rates. Therefore, cover systems that minimize infiltration appear to have greater value for reducing the volume of acid that drains from the blocks, compared to decreasing acid production rates within the block.

Therefore, a cover

6.2.2 Temperature-controlled storage

In cold climates such as the one in this study, it is not expected that H_2SO_4 production will decrease if the interior temperature of a block gradually cools with time.

Because the majority of H₂SO₄ is produced in the upper 1 m as a result of increased summer temperatures, cooling of the interior of the block to the average annual mean temperature (0.7°C) will have little effect on the overall production of H₂SO₄.

Maintaining low temperatures (<5°C) within S⁰ blocks is a potentially effective strategy for minimizing H₂SO₄ production rates. However, insulating covers must be designed carefully. For example, an insulating cover may maintain block temperatures relatively cool in the summer but relatively warm in the winter. Overall, the change in annual H₂SO₄ produced may be negligible. The exothermic nature of S⁰ oxidation should also be considered when designing insulating covers. Heat released during S⁰ oxidation could be trapped in the block and increase temperatures, and H₂SO₄ production rates, with time.

6.2.3 Biocide application

Biocide application to the surface of S⁰ blocks may appear to be a potentially effective method for reducing H₂SO₄ production given the prevalence of near-surface H₂SO₄ production. Surficial biocide application may limit near-surface S⁰ oxidation, however this might increase O₂ availability for H₂SO₄ production at greater depths. The end result may be similar annual H₂SO₄ production but with S⁰ oxidation occurring at greater depths within the block.

6.2.4 Cover systems

Cover systems that limit O₂ influx would be an effective method for minimizing H₂SO₄ production in S⁰ blocks (limiting influx of H₂O discussed in 6.2.1). The [O₂] in the blocks decreased to less than 1% and S⁰ oxidation was a zero-order reaction (no rate dependence if [O₂] > ~1%); therefore, any decrease in [O₂] at the surface of a S⁰ block will proportionally decrease the amount of H₂SO₄ produced in the blocks.

Soil covers are one technique for limiting O₂ and H₂O influx to materials produced at mines. Soil cover layers that maintain near-saturated conditions are resistant to gas diffusion and are used to minimize the diffusive influx of atmospheric O₂. A capillary break in a layered soil cover may be created by constructing the layer with high saturations directly on the relatively well-drained, hydrophobic, and highly permeable S⁰. Pore-water H₂SO₄ concentrations (i.e. RH < 100%) in the S⁰ create the potential for diffusive vapour flux from soil covers (saturated vapour pressure) to the underlying S⁰. The contribution of water vapour diffusion in the overall water balance of a S⁰ block soil cover may be negligible when precipitation exceeds evapotranspiration, but may be important in more arid environments.

ACKNOWLEDGEMENTS

The authors acknowledge Syncrude Canada Ltd., the University of Saskatchewan, and NSERC for financial support. Ron Lewko (Syncrude Canada Ltd.), and

Robert Mahood and Gord McKenna (formerly of Syncrude Canada Ltd.) provided technical and project management support. Julie Robertson, Rob Holben, Sean Shaw, Ray Kirkland, and Matt Harker (U of S) provided field and lab support.

REFERENCES

- Baker, B.J., M.A. Lutz, S.C. Dawson, P.L. Bond, and J.F. Banfield. 2004. Metabolically active eukaryotic communities in extremely acidic mine drainage. *Appl. Environ. Microbiol.* 70: 6264–6271.
- Birkham, T.K., M.J. Hendry, S.L. Barbour, S.K. Carey, J.R. Lawrence, and R. Lewko. 2010a. Water flow and storage in fractured, unsaturated sulphur blocks. *Submitted to Can. Geotech. J., June 2009.*
- Birkham, T.K., M.J. Hendry, and S.L. Barbour. 2010b. Advective and diffusive gas transport through fractured sulphur blocks. *Vadose Zone Journal* 9: 451-461.
- Birkham T.K., M.J. Hendry, and S.L. Barbour. 2010c. Controls and rates of acid production in commercial-scale sulphur blocks. *Journal of Environmental Quality* 39: 834-844.
- Bonstrom, K. 2007. Physical controls on water migration in elemental sulphur blocks. M.Sc. Thesis, Dept. Geological Sciences, University of Saskatchewan. Saskatoon, SK, Canada.
- Bonstrom, K., S.L. Barbour, and M.J. Hendry. 2009. Physical and hydraulic characterization of fractured, hydrophobic, sulphur within above ground sulphur blocks. Under revision, *Can. Geotech. J.*
- Energy Resources and Conservation Board (ERCB) (Alberta, Canada). 2008. Alberta's energy reserves 2007 and supply/demand outlook 2008-2017. ST98-2008.
- Environment Canada, 2009a. Accessed June 3. http://www.climate.weatheroffice.ec.gc.ca/climate_normals/results_e.html?StnID=2519&autofwd=1
- Fredlund, D.G. and H. Rahardjo. 1993. Soil mechanics for unsaturated soils. John Wiley&Sons Inc., Toronto, ON.
- Janzen, H.H. and J.R. Bettany. 1987a. Measurement of sulphur oxidation in soils. *Soil Sci.* 144: 444–452.
- Kosich, D. 2008. Sulphur, potash prices soar last month as base and precious metals decline. *International business times*, June 20.
- Lawrence, J.R. and J.J. Germida. 1988. Relationship between microbial biomass and elemental sulfur oxidation in agricultural soils. *Soil Sci. Soc. Am. J.* 52(3): 672–677.
- Moldrup P, T Olesen, S Yoshikawa, T Komatsu, and DE Rolston. 2004. Three-porosity model for predicting the gas diffusion coefficient in undisturbed soil. *Soil Science Society of America Journal* 68: 750-759.
- Moslet, P.O. 2007. Field testing of uniaxial compression strength of columnar sea ice. *Cole Reg. Sci. Technol.* 48: 1–14.
- Nordstrom, D.K., C.N. Alpers, C.J. Ptacek, and D.W. Blowes. 2000. Negative pH and extremely acidic mine waters from Iron Mountain, California. *Environ. Sci. Technol.* 34: 254–258.

- Ober J.A. 2002. Materials flow of sulfur. U.S. Geological Survey. Open-file report 02-298.
- Ober J.A. July, 2009. U.S. Geological Survey, 2007 Minerals Yearbook: Sulfur.
- Pisz, J. 2008. Characterization of extremophilic sulphur oxidizing microbial communities inhabiting the sulphur blocks of Alberta's oil sands. M.Sc. Thesis, Dept. Soil Science, College of Agriculture, University of Saskatchewan, Saskatoon, SK.
- Plummer, L.N., D.L. Parkhurst, G.W. Fleming, and S.A. Dunkle. 1988. U.S. Geol. Survey Water-Resour. Invest. Report 88-4153.
- Proce, B. 2006. Oilsands Review. October 2006, 42–45.
- Severinghaus, J.P., M.L. Bender, R.F. Keeling, and W.S. Broecker. 1996. Fractionation of soil gases by diffusion of water vapor, gravitational settling, and thermal diffusion. *Geochim. Cosmochim. Acta* 60(6): 1005–1018.
- Syncrude Canada Ltd. 2004a. Geo-environmental observations of 17 sulphur blocks in Alberta. Research Dept. Progress Report 33(2).
- Syncrude Canada Ltd. 2004b. Geochemical characterization of a large sulphur block at Syncrude: results from the 2003 field investigation. June 21, 2004.
- Weast, R.C. and M.J. Astle. 1981. CRC Handbook of Chemistry and Physics. CRC Press, Boca Raton, FL.
- Wilson, G.W., D.G. Fredlund, and S.L. Barbour. 1997. The effect of soil suction on evaporative fluxes from soil surfaces. *Can. Geotech. J.* 34: 145–155.